DALTON

Syntheses and quadratic hyperpolarizabilities of some (pyridylalkynyl)metal complexes: crystal structures of [Ni{2-(C≡C)$C_5H_3NNO_2$-5}(PPh_3)(η-C_5H_5)], [Au{2-(C≡C)$C_5H_3NNO_2$-5}(PPh_3)] and [Au{2-(C≡C)C_5H_4N}(PPh_3)]‡

Raina H. Naulty,[a] Marie P. Cifuentes,[a] Mark G. Humphrey,*,†,[a] Stephan Houbrechts,[b] Carlo Boutton,[b] André Persoons,[b] Graham A. Heath,[c] David C. R. Hockless,[c] Barry Luther-Davies[d] and Marek Samoc[d]

[a] *Department of Chemistry, Australian National University, Canberra, ACT 0200, Australia*
[b] *Centre for Research on Molecular Electronics and Photonics, Laboratory of Chemical and Biological Dynamics, University of Leuven, Celestijnenlaan 200D, B-3001 Leuven, Belgium*
[c] *Research School of Chemistry, Australian National University, Canberra, ACT 0200, Australia*
[d] *Australian Photonics Cooperative Research Centre, Laser Physics Centre, Research School of Physical Sciences and Engineering, Australian National University, Canberra, ACT 0200, Australia*

The complexes [Ru{2-(C≡C)C_5H_3NR-5}$(PPh_3)_2$(η-C_5H_5)] (R = NO_2 **1** or H **2**), [Ni{2-(C≡C)C_5H_3NR-5}(PPh_3)(η-C_5H_5)] (R = NO_2 **3** or H **4**) and [Au{2-(C≡C)C_5H_3NR-5}L] (L = PPh_3, R = NO_2 **5** or H **6**; L = PMe_3, R = NO_2 **7**) have been synthesized and **3**, **5** and **6** structurally characterized; no significant increase in quinoidal vinylidene contribution to the acetylide ground-state structure is apparent on progression from structurally characterized phenylacetylide complexes to the new pyridylacetylide complexes, or upon replacement of 5-H by 5-NO_2 in progressing from **6** to **5**. The molecular quadratic optical non-linearities of **1**–**7** have been determined by hyper-Rayleigh scattering (HRS). The HRS measurements at 1064 nm are consistent with an increase in β upon replacement of phenyl by an N-heterocyclic ring (replacing a nitrophenylacetylide by a nitropyridylacetylide ligand) for the ruthenium and gold systems, but with no change for the nickel complexes, and with an increase in non-linearity upon replacement of PMe_3 by PPh_3 in progressing from **7** to **5**. The bulk second-order susceptibilities of the series have been determined by Kurtz powder measurements at 1064 nm, with the only significant response (about eight times that of urea) being that of **3**; this complex was the only one of the three structurally characterized to pack non-centrosymmetrically in the crystal lattice. Electrochemical data for **1**–**4** have been obtained; comparison to analogous nitrophenylacetlylide complexes reveals that replacing nitrophenylacetylide by nitropyridylacetylide leads to a significant increase in $M^{II/III}$ oxidation potential for the ruthenium complexes, but to no change for the nickel examples. The parameter $E°_{M^{II/III}} - E°_{NO_2/NO_2^-}$ was evaluated for **1**–**4**, results for M = Ru *vs.* Ni being consistent with experimentally determined non-linearities, *i.e.* smaller $\Delta E°$ and larger non-linearities for ruthenium *vs.* nickel.

The optical non-linearities of organometallic complexes have been investigated intensively recently.[2] Our focus in this area has been on metal σ-acetylide complexes with the donor–bridge–acceptor composition shown to produce enhanced non-linear optical (NLO) responses in organic molecules.[1,3] We have probed the effect of varying metal and coligand at the ligated metal donor group, the significance of chain lengthening of the σ-acetylide ligand by various bridging functionalities, and the importance of the nitro acceptor group on both quadratic and cubic NLO performance, and have recently commented on the significance of metal valence electron count and oxidizability on quadratic NLO merit, in the process defining 'figures of merit' for several ligand metal centres.

Our studies have thus far focused on σ-phenylacetylide complexes. However, organic compounds where the phenyl rings are replaced by heterocyclic groups such as thiophene-2,5-diyl or furyl have been reported to give increased second-order responses. For example, Dirk *et al.*[4] examined chromophores in which the phenyl ring of the bridge was replaced with a thiazolyl group, noting an improved quadratic non-linearity, β, relative to that of the prototypical organic NLO material 4-(dimethylamino)-4′-nitrostilbene (dans); this was attributed to the decreased aromaticity of the heterocyclic ring compared to that of the phenyl group. Cheng *et al.*[5] examined chromophores in which a phenyl ring of the bridge was replaced with a furyl or thiophenyl ring, observing bathochromic shifts in the optical absorption spectra and enhanced hyperpolarizabilities compared to those of the aromatic analogues. Replacement of both of the phenyl rings in an analogue of dans with thiophene-2,5-diyl groups resulted in a two-fold increase in the product of the dipole moment and quadratic non-linearity, μβ.[6] Given these precedents in organic chemistry, it seems logical to examine the NLO merit of heterocyclic σ-acetylide complexes. This paper reports syntheses, spectroscopic and, in some instances, X-ray structural and electrochemical characterization of new σ-pyridylacetylide complexes, their molecular quadratic optical non-linearities at 1064 nm and two-level-corrected values as determined by hyper-Rayleigh scattering (HRS), and their bulk second-order susceptibilities at 1064 nm measured by the Kurtz powder technique, together with comparisons with previously reported data for the analogous σ-phenylacetylide complexes.

Experimental

General

All reactions were carried out under an atmosphere of nitrogen

---

† E-Mail: mark.humphrey@anu.edu.au

‡ Organometallic complexes for non-linear optics. Part 13.[1]

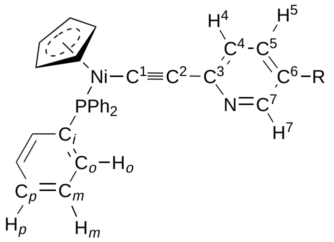

Scheme 1 Numbering scheme for NMR spectral assignments of complexes **3** ($R = NO_2$) and **4** ($R = H^6$). Analogous schemes for 2-$(HC{\equiv}C)C_5H_4N$ **I**, 2-$(Me_3SiC{\equiv}C)C_5H_3NNO_2$-5 **II**, [Ru{2-$(C{\equiv}C)C_5H_3$-NR-5}$(PPh_3)_2$(η-$C_5H_5$)] and [Au{2-$(C{\equiv}C)C_5H_3NR$-5}$(PPh_3)$]

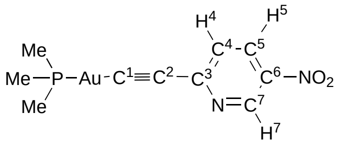

Scheme 2 Numbering scheme for NMR spectral assignments of [Au{2-$(C{\equiv}C)C_5H_3NNO_2$-5}(PMe_3)] **7**

with the use of standard Schlenk techniques;[7] no attempt was made to exclude air during work-up of products. Solvents were dried as follows: dichloromethane by distilling over CaH_2, methanol by distilling over magnesium activated with I_2, toluene by distilling over sodium–benzophenone, and diethyl ether by distilling over sodium–benzophenone; other solvents were used as received. Column chromatography was carried out using Merck aluminium oxide 90 active basic (activity stage III, 70–230 mesh ASTM, with 10 cm columns). Light petroleum refers to a fraction of boiling range 60–80 °C.

The following compounds were prepared by literature methods: 2-ethynylpyridine,[8] [$NiCl(PPh_3)$(η-C_5H_5)],[9] [RuCl-$(PPh_3)_2$(η-C_5H_5)],[10] [$PdCl_2(PPh_3)_2$][11] and [$AuCl(PPh_3)$];[12] [$AuCl(PMe_3)$][13] was provided by Dr. Mark Brown, Research School of Chemistry, Australian National University. Copper(I) iodide (Aldrich), 2-bromo-5-nitropyridine (Aldrich), trimethylsilylacetylene (Aldrich) and triethylamine (BDH) were used as received.

Microanalyses were performed at the Research School of Chemistry, Australian National University. Infrared spectra were recorded as solutions in 0.1 mm CaF_2 cells using a Perkin-Elmer System 2000 FT-IR spectrometer, and UV/VIS spectra as tetrahydrofuran (thf) solutions using a Cary 5 spectrophotometer. Mass spectra were recorded using a VG ZAB 2SEQ instrument (30 kV Cs^+ ions, current 1 mA, accelerating potential 8 kV, 3-nitrobenzyl alcohol matrix) at the Research School of Chemistry, Australian National University; peaks are reported as *m*/*z* (assignment, relative intensity). Electrochemical measurements were carried out using a Princeton Applied Research model 170 potentiostat. The supporting electrolyte was $[NBu^n_4][PF_6]$ (0.5 mol dm^{-3}) in distilled deoxygenated dichloromethane. Solutions (1×10^{-3} mol dm^{-3}) were made under a purge of nitrogen and measured *versus* an Ag–AgCl reference electrode at −50 °C, such that the ferrocene–ferrocenium redox couple was located at +0.55 V.

Proton, ^{13}C and ^{31}P NMR spectra were recorded using a Varian Gemini-300 FT NMR spectrometer and are referenced to residual $CHCl_3$ (δ 7.24), $CDCl_3$ (δ 77.0) and external 85% H_3PO_4 (δ 0.0), respectively. All carbon and phosphorus NMR spectra are broad-band proton decoupled, and coupling constants are quoted as absolute values. The NMR spectral assignments follow the numbering schemes shown in Schemes 1 and 2.

Characterization of 2-$(HC{\equiv}C)C_5H_4N$ I[8]

This compound was found to be highly unstable in air; it was stored as a solution in diethyl ether. $\tilde{\nu}_{max}/cm^{-1}$ $(CH_2Cl_2) = 2108$ (C≡C). $\delta_H(CDCl_3)$ 3.13 (1 H, s, ≡CH), 7.25 (1 H, m, H^6), 7.46 [1 H, d, ^3J(HH) 2, H^4], 7.65 [1 H, td, ^3J(HH) 2, ^4J(HH) 1, H^5] and 8.58 [1 H, d, ^3J(HH) 1 Hz, H^7]. $\delta_C(CDCl_3)$ 82.7 (C^2), 103.0 (C^1), 127.5 (C^4), 128.4 (C^5), 136.2 (C^3), 142.3 (C^7) and 150.0 (C^6).

Syntheses

2-$(Me_3SiC{\equiv}C)C_5H_3NNO_2$-5 II. 2-Bromo-5-nitropyridine (1.00 g, 4.54 mmol), trimethylsilylacetylene (0.60 cm^3, 0.42 g, 4.3 mmol), CuI (5 mg, 0.03 mmol) and [$PdCl_2(PPh_3)_2$] (73 mg, 0.22 mmol) were added to deoxygenated triethylamine (20 cm^3). The reaction mixture was stirred for 3 h, after which time the triethylamine was removed, and the crude product extracted into dichloromethane and adsorbed onto alumina. Column chromatography, performed using 20% dichloromethane–80% light petroleum as eluent, afforded 830 mg (77%) of white crystals (Found: C, 54.90; H, 5.46; N, 12.32. $C_{10}H_{12}N_2O_2Si$ requires C, 54.52; H, 5.49; N, 12.72%). $\tilde{\nu}_{max}/cm^{-1}$ $(CH_2Cl_2) =$ 2061 (C≡C). $\delta_H(CDCl_3)$ 1.56 (9 H, s, Me), 7.60 [1 H, d, ^3J(HH) 9, H^4], 8.43 [1 H, dd, ^3J(HH) 9, ^4J(HH) 3, H^5] and 9.37 [1 H, d, ^4J(HH) 3 Hz, H^7]. $\delta_C(CDCl_3)$ 0.6 (s, Me), 82.3 (C^2), 101.8 (C^1), 127.2 (C^4), 131.3 (C^5), 142.6 (C^3), 145.3 (C^7) and 148.1 (C^6). *m*/*z* 220 (M^+, 17), 205 (100, $[M - Me]^+$) and 159 (23%, $[M - Me - NO_2]^+$).

[Ru{2-$(C{\equiv}C)C_5H_3NNO_2$-5}$(PPh_3)_2$(η-C_5H_5)] 1. A mixture of [$RuCl(PPh_3)_2$(η-C_5H_5)] (300 mg, 0.41 mmol) and compound **II** (132 mg, 0.60 mmol) was refluxed in a methanolic solution of NaOMe (30 cm^3 methanol, 15 mg sodium) for 1 h, and the resultant solution allowed to cool to room temperature. The solvent was removed *in vacuo* and the residue adsorbed onto alumina. Elution with 50% acetone–50% dichloromethane afforded a red solution; light petroleum was added and the product precipitated by reducing the solvent volume on a rotary evaporator. Upon filtering, 155 mg of a red powder (44%) was isolated (Found: C, 68.02; H, 4.89; N, 3.40. $C_{48}H_{38}N_2O_2P_2Ru{\cdot}0.5C_3H_6O$ requires C, 68.58; H, 4.77; N, 3.23%). λ_{max}/nm (thf) 468 (ε/dm^3 mol^{-1} cm^{-1} 17 400). $\tilde{\nu}_{max}/cm^{-1}$ $(CH_2Cl_2) =$ 2029 cm^{-1} (C≡C). $\delta_H(CDCl_3)$ 2.14 (3 H, s, Me_2CO), 4.42 (5 H, s, C_5H_5), 6.50 [1 H, d, ^3J(HH) 9, H^4], 7.07 [12 H, t, *J*(HH) 7 Hz, H_m], 7.19 (6 H, m, H_p), 7.33 (12 H, m, H_o), 8.02 [1 H, dd, ^3J(HH) 9, ^4J(HH) 3, H^5] and 9.25 [1 H, d, ^4J(HH) 3 Hz, H^7]. $\delta_C(CDCl_3)$ 86.3 (C_5H_5), 121.5 (C^2), 124.8 (C^4), 127.4 (C_m), 128.8 (C_p), 129.8 (C^5), 133.5 (C_o), 137.8 (m, C_i), 145.9 (C^7); carbon atoms C^1, C^3 and C^6 were not detected. $\delta_P(CDCl_3)$ 51.2. *m*/*z* 838 (M^+, 37), 691 {9, [M − 2-$(C{\equiv}C)C_5H_3NNO_2$-5$]^+$}, 576 (43, $[M - PPh_3]^+$) and 429 {100%, [*M* − 2-$(C{\equiv}C)C_5H_3NNO_2$-5 − $PPh_3]^+$}.

[Ru{2-$(C{\equiv}C)C_5H_4N$}$(PPh_3)_2$(η-C_5H_5)] 2. A solution of compound **I** in ether (2 cm^3, 0.1 mol dm^{-3}) was transferred to a Schlenk tube and the ether removed *in vacuo*. Methanol (20 cm^3) was added immediately *via* a cannula. The complex [RuCl-$(PPh_3)_2$(η-C_5H_5)] (200 mg, 0.28 mmol) was added to the resultant solution and the mixture heated at reflux for 30 min. The chloro complex gradually dissolved to give a bright orange solution, which was then allowed to cool. Sodium (10 mg, 0.43 mmol) was added, whereupon a yellow precipitate formed, which was filtered off and washed with methanol and light petroleum. Yield 188 mg (83%) (Found: C, 71.65; H, 5.05; N, 1.64. $C_{48}H_{39}NP_2Ru{\cdot}0.5CH_4O$ requires C, 72.02; H, 5.11; N, 1.73%). λ_{max}/nm (thf) 331 (ε/dm^3 mol^{-1} cm^{-1} 14 500). $\tilde{\nu}_{max}/cm^{-1}$ (CH_2Cl_2) 2070 (C≡C). $\delta_H(CDCl_3)$ 3.48 (1.5 H, s, MeOH), 4.35 (5 H, s, C_5H_5), 6.65 [1 H, d, ^3J(HH) 7, H^4], 6.82 [1 H, t, ^3J(HH) 7, H^5], 7.07 [12 H, t, *J*(HH) 7, H_m], 7.18 (6 H, m, H_p), 7.43 (12 H, m, H_o), 8.41 [1 H, d, ^3J(HH) 4 Hz, H^7]; resonance for H^6 is obscured by those of H_m and H_p. $\delta_C(CDCl_3)$ 85.6 (C_5H_5), 117.8 (C^2), 125.6 (C^4), 127.3 (C_m), 128.4 (C_p), 133.7 (C_o), 138.7 (C_i); carbon atoms C^1, C^3, C^5, C^6 and C^7 were not detected due to poor signal/noise. $\delta_P(CDCl_3)$ 51.4. *m*/*z* 793 (M^+, 35), 691

{6, [M − 2-(C≡C)C_5H_4N]$^+$}, 531 (47, [M − PPh_3]$^+$) and 429 {100%, [M − 2-(C≡C)C_5H_4N − PPh_3]$^+$}.

[Ni{2-(C≡C)$C_5H_3NNO_2$-5}(PPh_3)(η-C_5H_5)] 3. A mixture of [NiCl(PPh_3)(η-C_5H_5)] (120 mg, 0.29 mmol), compound **II** (66 mg, 0.30 mmol) and CuI (5 mg, 0.03 mmol) was stirred in triethylamine (20 cm^3) containing NaOMe in methanol (3.0 cm^3, 0.22 mol dm^{-3}) for 16 h. The solvent was removed under reduced pressure, the residue extracted with dichloromethane (40 cm^3), and the extract adsorbed onto alumina. Column chromatography with dichloromethane as eluent afforded a brown band; addition of light petroleum (10 cm^3) and ethanol (2 cm^3) to the eluate and removal of the dichloromethane precipitated the microcrystalline product which was filtered off (90 mg, 58%) (Found: C, 67.56; H, 4.21; N, 5.00. $C_{30}H_{23}N_2NiO_2P$ requires C, 67.58; H, 4.35; N, 5.25%). λ_{max}/nm (thf) 456 (ε/dm^3 mol^{-1} cm^{-1} 11 000). $\tilde{\nu}_{max}$/cm^{-1} 2086 (C≡C). δ_H($CDCl_3$) 5.24 (5 H, s, C_5H_5), 6.02 [1 H, d, ^3J(HH) 9, H^4], 7.40 (9 H, m, H_m, H_p), 7.69 (6 H, m, H_o), 7.88 [1 H, dd, ^3J(HH) 9, ^4J(HH) 2, H^5] and 9.08 [1 H, d, ^4J(HH) 2 Hz, H^7]. δ_C($CDCl_3$) 93.1 (C_5H_5), 113.6 [d, J(CP) 45, C^1], 120.7 (C^2), 125.6 (C^4), 128.3 [d, J(CP) 10, C_m], 129.9 (C^5), 130.5 (C_p), 133.5 [d, J(CP) 58, C_i], 133.9 [d, J(CP) 11 Hz, C_o], 139.9 (C^3), 145.1 (C^7) and 150.4 (C^6). δ_P($CDCl_3$) 43.2. m/z 533 (M^+, 26), 385 {19, [M − 2-(C≡C)$C_5H_3NNO_2$-5]$^+$} and 320 {16, [M − 2-(C≡C)$C_5H_3NNO_2$-5 − C_5H_5]$^+$}.

[Ni{2-(C≡C)C_5H_4N}(PPh_3)(η-C_5H_5)] 4. A solution of compound **I** in ether (6.5 cm^3, 0.1 mol dm^{-3}) was collected and the ether removed. Triethylamine (10 cm^3) was added immediately *via* a cannula, [NiCl(PPh_3)(η-C_5H_5)] (200 mg, 0.47 mmol) and CuI (5 mg, 0.03 mmol) were added and the resultant mixture stirred for 16 h. The reaction mixture was then adsorbed onto alumina and subjected to column chromatography with 50% dichloromethane–50% light petroleum as eluent. The green solution collected was reduced to dryness. Addition of ether and light petroleum afforded a green microcrystalline solid, yield 99 mg (42%). This complex decomposes slowly in solution over a period of hours, preventing recrystallization; satisfactory microanalyses could not be obtained. λ_{max}/nm (thf) 413 (ε/dm^3 mol^{-1} cm^{-1} 1400). $\tilde{\nu}_{max}$/cm^{-1} 2101 (C≡C). δ_H($CDCl_3$) 5.22 (5 H, s, C_5H_5), 6.03 [1 H, d, ^3J(HH) 8 Hz, H^4], 6.75 (m, H^5), 7.12 (m, H^6), 7.38 (9 H, m, H_m, H_p), 7.72 (6 H, m, H_o) and 8.25 (m, H^7). δ_C($CDCl_3$) 92.8 (C_5H_5), 119.3 (C^2), 125.9 (C^4), 128.2 [d, J(CP) 10, C_m], 130.1 (C^5), 130.2 (C_p), 133.9 [d, J(CP) 11, C_o], 134.0 [d, J(CP) 48 Hz, C_i], 134.9 (C^3), 146.0 (C^7) and 148.7 (C^6). δ_P($CDCl_3$) 42.3. m/z 487 (M^+, 79), 385 {44, [M − 2-(C≡C)-C_5H_4N]$^+$} and 320 {28%, [M − 2-(C≡C)C_5H_4N − C_5H_5]$^+$}.

[Au{2-(C≡C)$C_5H_3NNO_2$-5}(PPh_3)] 5. A mixture of [AuCl(PPh_3)] (120 mg, 0.24 mmol) and compound **II** (70 mg, 0.32 mmol) in a solution of NaOMe in methanol (10 cm^3, 0.10 mol dm^{-3}) was stirred for 16 h, after which time a pale yellow solid had precipitated and was filtered off. Recrystallization was effected by extraction into dichloromethane, addition of ether, partial removal of solvent on a rotary evaporator and filtration to yield 93 mg (64%) (Found: C, 48.97; H, 2.69; N, 4.67. $C_{25}H_{18}AuN_2O_2P$ requires C, 49.52; H, 2.99; N, 4.62%). λ_{max}/nm (thf) 339 (ε/dm^3 mol^{-1} cm^{-1} 25 600). $\tilde{\nu}_{max}$/cm^{-1} 2123 (C≡C). δ_H($CDCl_3$) 7.45–7.52 (16 H, m, Ph, H^4), 8.33 [1 H, dd, ^3J(HH) 9, ^4J(HH) 3, H^5] and 9.32 [1 H, d, ^4J(HH) 3 Hz, H^7]. δ_C($CDCl_3$) 102.4 [d, J(CP) 26, C^1], 126.7 (C^4), 129.3 [d, J(CP) 60, C_i], 129.4 [d, J(CP) 11, C_m], 130.9 (C^5), 131.7 (C_p), 134.3 [d, J(CP) 14 Hz, C_o], 141.6 (C^3), 145.3 (C^7), 149.8 (C^6); C^2 not observed. δ_P($CDCl_3$) 42.3. m/z 721 {41, [Au$(PPh_3)_2$]$^+$}, 606 (21, [M + H]$^+$) and 459 {100, [M − 2-(C≡C)$C_5H_3NNO_2$-5]$^+$}.

[Au{2-(C≡C)C_5H_4N}(PPh_3)] 6. A solution of compound **I** in ether (4 cm^3, 0.1 mol dm^{-3}) was transferred to a Schlenk tube and the ether removed. Methanol (20 cm^3) was added immediately *via* a cannula. To this solution was added [AuCl(PPh_3)] (200 mg, 0.40 mmol) and sodium (*ca.* 40 mg, excess). The solution was allowed to stir for 16 h and the solvent was then removed *in vacuo*. Addition of a small amount of methanol afforded 130 mg (58%) of a pale microcrystalline solid (Found: C, 53.46; H, 3.27; N, 2.38. $C_{25}H_{19}AuNP$ requires C, 53.49; H, 3.41; N, 2.50%). λ_{max}/nm (thf) 300 (ε/dm^3 mol^{-1} cm^{-1} 20 800). $\tilde{\nu}_{max}$/cm^{-1} 2123 (C≡C). δ_H($CDCl_3$) 7.07 (2 H, m, H^4, H^6), 7.41–7.55 (16 H, m, Ph, H^5) and 8.50 (1 H, m, H^7). δ_C($CDCl_3$) 103.1 [d, J(CP) 26, C^1], 121.3 (C^2), 126.9 (C^4), 129.1 [d, J(CP) 11, C_m], 130.0 (C^5), 131.6 (C_p), 134.3 [d, J(CP) 14 Hz, C_o], 135.4 (C^3), 144.5 (C^7), 149.6 (C^6); C_i partially obscured by C_m. δ_P($CDCl_3$) 42.7. m/z 1020 {37, [M + Au(PPh_3)]$^+$}, 721 {35, [Au$(PPh_3)_2$]$^+$}, 562 (61, [M + H]$^+$) and 459 (100, [M − C≡CC_5H_3N]$^+$).

[Au{2-(C≡C)$C_5H_3NNO_2$-5}(PMe_3)] 7. Copper(I) iodide (5 mg, 0.03 mmol) and a solution of NaOMe in methanol (8 cm^3, 0.3 mol dm^{-3}) were added to a mixture of [AuCl(PMe_3)] (85 mg, 0.27 mmol) and compound **II** (60 mg, 0.27 mmol) in dichloromethane (10 cm^3), and the resultant mixture allowed to stir for 16 h. The solvent was removed under reduced pressure and the yellow product crystallized from methanol, yield 83 mg (72%) (Found: C, 28.64; H, 2.75; N, 6.88. $C_{10}H_{12}AuN_2O_2P$ requires C, 28.59; H, 2.88; N, 6.67%). λ_{max}/nm (thf) 340 (ε/dm^3 mol^{-1} cm^{-1} 16 500). $\tilde{\nu}_{max}$/cm^{-1} 2121 (C≡C). δ_H($CDCl_3$) 1.54 (9 H, m, Me), 7.48 [1 H, d, ^3J(HH) 9, H^4], 8.31 [1 H, dd, ^3J(HH) 9, ^4J(HH) 3, H^5] and 9.30 [1 H, d, ^4J(HH) 3 Hz, H^7]. δ_C($CDCl_3$) 15.6 [d, J(CP) 36 Hz, Me], 103.1 (br, C^1), 126.9 (C^4), 130.8 (C^5), 141.6 (C^3), 145.3 (C^7), 149.9 (C^6); C^2 not observed. δ_P($CDCl_3$) 1.3. m/z 693 {15, [Au(PMe_3) + M]$^+$}, 421 (58, [M + H]$^+$), 349 (100, [Au$(PMe_3)_2$]$^+$) and 273 {87, [M − 2-(C≡C)$C_5H_3NNO_2$-5]$^+$}.

Crystallography

Crystals of complexes **3**, **5** and **6** suitable for diffraction analyses were grown by slow diffusion of hexane into dichloromethane at room temperature (**5**, **6**) or 268 K (**3**). Unique diffractometer data sets were obtained using an ω–2θ scan mode at 296 K and yielded N independent reflections, N_o of these with $I \geqslant 3.00\sigma(I)$ being considered 'observed' and used in full-matrix least-squares refinement. An empirical ψ-type absorption correction was applied in each case; no decay corrections were required. Anisotropic thermal parameters were refined for the non-hydrogen atoms; $(x, y, z, U_{iso})_H$ were included constrained at estimated values. Conventional residuals R and R' on $|F|$ are given; the weighting function $w = 1/\sigma^2(F_o)$ [where $\sigma^2(F_o) = \sigma_c^2(F_o) + (p^2/4)F_o^2$, $\sigma_c(F_o)$ = estimated standard deviation (e.s.d.) based on counting statistics and p = p factor determined experimentally from standard reflections] was employed. Computation used the TEXSAN package.[14] Specific data collection, solution and refinement parameters are given in Table 1. Pertinent results are given in the figures and tables.

CCDC reference number 186/708.

HRS Measurements

An injection-seeded Nd–YAG laser (Q-switched Nd–YAG Quanta Ray GCR5, 1064 nm, 8 ns pulse, 10 Hz) was focused into a cylindrical cell (7 cm^3) containing the sample. The intensity of the incident beam was varied by rotation of a half-wave plate placed between crossed polarizers. Part of the laser pulse was sampled by a photodiode to measure the vertically polarized incident light intensity. The frequency-doubled light was collected by an efficient condenser system and detected by a photomultiplier. The harmonic scattering and linear scattering were distinguished by appropriate filters; gated integrators were used to obtain intensities of the incident and harmonic scattered light. All measurements were performed in thf using p-nitroaniline ($\beta = 21.4 \times 10^{-30}$ esu; 1 esu = 2.7×10^{20} C m^3 V^{-1})

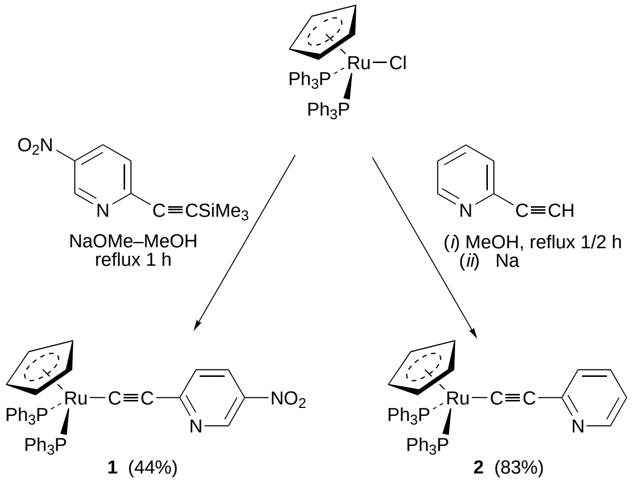

Scheme 3

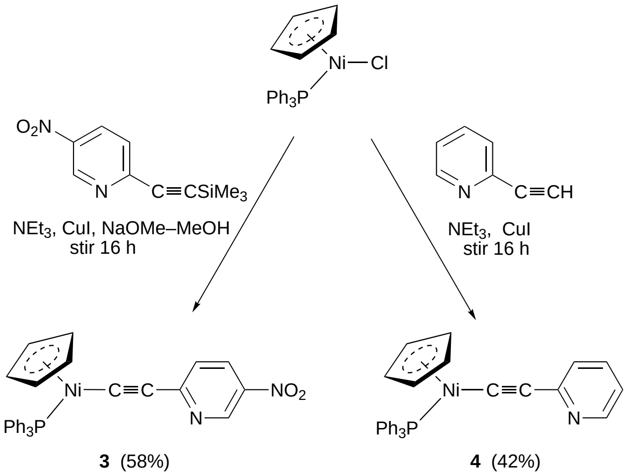

Scheme 4

as a reference.[15] Further details of the experimental procedure have been reported elsewhere.[16]

Kurtz powder measurements

Samples were unsized microcrystalline powders placed in the circular cavity (10 mm diameter × 0.5 mm depth) of a microscope slide with a cover slip. The fundamental output of a Quanta-Ray GC-130 Nd–YAG laser was directed onto the sample (spot size ≈ 5 mm, power ≈ 20 mJ). A collecting lens (orthogonally placed with respect to the fundamental beam) focused the backscattered second harmonic light through an infrared absorbing filter and a 532 nm interference filter onto a photodiode detector which was connected to a Hewlett-Packard digital 54510A oscilloscope. Measurements thus made were compared with those for a urea powder sample.

Results and Discussion

Syntheses of acetylenes

2-Pyridylacetylene **I** was prepared by the literature procedure,[8] namely $[PdCl_2(PPh_3)_2]$/CuI-catalysed coupling of 2-bromopyridine with trimethylsilylacetylene, followed by deprotection of the intermediate pyridyl(trimethylsilyl)acetylene with base [we also investigated reaction of 2-bromopyridine with (the less expensive) 2-methylbut-3-yn-2-ol which proceeded to afford $Me_2C(OH)C{\equiv}CC_5H_4N$-2, but we were unable to deprotect this successfully]. Analogous palladium–copper catalysed reaction of 2-bromo-5-nitropyridine with trimethylsilylacetylene afforded 2-$(Me_3SiC{\equiv}C)C_5H_3NNO_2$-5 **II** in excellent yield. However, attempted deprotection of **II** with base afforded a dark oil, the analysis of which revealed that none of the desired 2-$(HC{\equiv}C)C_5H_3NNO_2$-5 was present. We then found that deprotection of **II** in the presence of the metal chloride afforded fair to good yields of the desired acetylide complexes, so isolation of 2-$(HC{\equiv}C)C_5H_3NNO_2$-5 was not pursued further.

Syntheses of σ-acetylide complexes

The synthetic methodologies employed for the preparation of the new σ-pyridylacetylide complexes are adaptations of those successfully utilized for the preparation of the corresponding σ-phenylacetylides.[3a,b,g,i,j] The (cyclopentadienyl)bis(triphenylphosphine)ruthenium σ-pyridylacetylide complexes were prepared in fair (**1**) or excellent (**2**) yield by reaction of the pyridylacetylene with $[RuCl(PPh_3)_2(\eta\text{-}C_5H_5)]$ and deprotonation of the intermediate vinylidene complex (Scheme 3). The (cyclopentadienyl)(triphenylphosphine)nickel σ-pyridylacetylide complexes **3** and **4** were prepared in good yields by reaction of $[NiCl(PPh_3)(\eta\text{-}C_5H_5)]$ with the pyridylacetylenes (Scheme 4). The pyridylacetylide complex **4** was unstable in solution, decomposing over a period of hours; we consequently investigated shorter reaction times for its synthesis, but these did not improve its yield. The (triphenylphosphine)gold σ-pyridylacetylide complexes **5** and **6** were prepared similarly to their σ-phenylacetylide analogues (Scheme 5), but the yield of the trimethylphosphine complex **7** was low by this methodology; the yield of **7** was increased substantially by addition of catalytic amounts of CuI to the reaction mixture (Scheme 6).

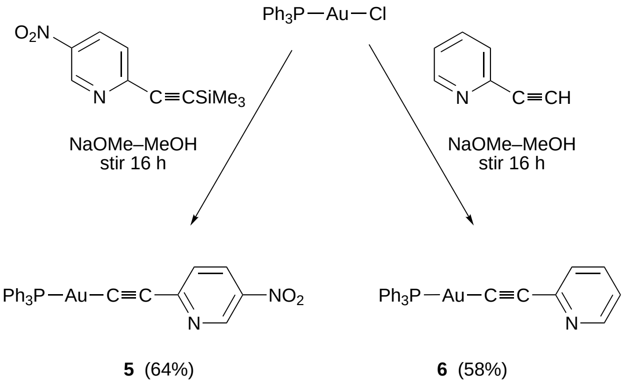

Scheme 5

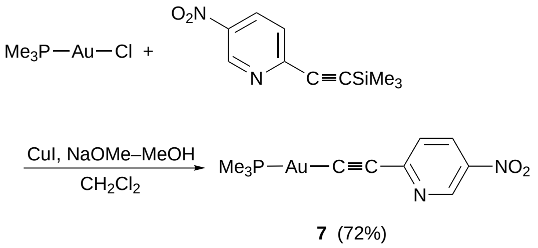

Scheme 6

The new σ-pyridylacetylide complexes were characterized by ^1H, ^{13}C, ^{31}P NMR, UV/VIS and IR spectroscopies, mass spectrometry, satisfactory microanalyses (with the exception of **4** which decomposes in solution over a period of hours preventing recrystallization: see above) and, in the case of **3**, **5** and **6**, single-crystal X-ray diffraction studies. Characteristic ν(C≡C) move to lower frequency for the ruthenium complexes on introduction of the nitro group [2070 (**2**), *cf.* 2029 cm^{-1} (**1**)], but this effect is attenuated in the nickel complexes [2101 (**4**), *cf.* 2086 cm^{-1} (**3**)], and disappears with the gold examples [2123 cm^{-1} (**5**, **6**)]. The ^1H, ^{13}C and ^{31}P NMR spectra are similar to those of previously reported phenylacetylide analogues, with the ^1H NMR spectra of **1**–**7** containing additional resonances assigned to pyridyl hydrogens between δ 5.2 and 9.1. The electron-withdrawing nitro and pyridyl N deshield H^7 significantly, leading to a resonance with a characteristic downfield shift and a

Table 1 Crystallographic data for complexes **3**, **5** and **6**

	3*	**5**	**6**
Empirical formula	$C_{30}H_{23}N_2NiO_2P$	$C_{25}H_{18}AuN_2O_2P$	$C_{25}H_{19}AuNP$
M	533.20	606.37	561.37
Crystal colour, habit	Orange, plate	Yellow, needle	Orange, plate
Crystal dimensions/mm	0.28 × 0.10 × 0.03	0.72 × 0.10 × 0.12	0.28 × 0.18 × 0.08
Crystal symmetry	Orthorhombic	Triclinic	Monoclinic
Space group	$Pna2_1$ (no. 33)	$P\bar{1}$ (no. 2)	$P2_1/n$ (no. 14)
a/Å	16.770(1)	8.885(3)	12.392(2)
b/Å	8.661(2)	17.346(3)	17.696(4)
c/Å	17.324(1)	22.809(4)	19.491(3)
α/°		78.86(2)	
β/°		78.87(2)	93.34(2)
γ/°		81.98(2)	
U/Å^3	2516.4(8)	3365(2)	4267(1)
Z	4	6	8
D_c/g cm^{-3}	1.407	1.795	1.748
μ/cm^{-1}	19.38 (Cu-Kα)	66.75 (Mo-Kα)	69.56 (Mo-Kα)
λ/Å	1.541 78	0.710 69	0.710 69
$2\theta_{max}$/°	120	50.1	50.1
Transmission factors	0.93–1.00	0.68–1.00	0.39–1.00
N	2181	11 941	7824
N_o [$I > 3.00\sigma(I)$]	1626	5604	4160
No. variables	325	838	505
p Factor	0.003	0.004	0.004
R	0.028	0.038	0.033
R'	0.022	0.030	0.024

* The absolute structure was checked; preferred residuals are quoted.

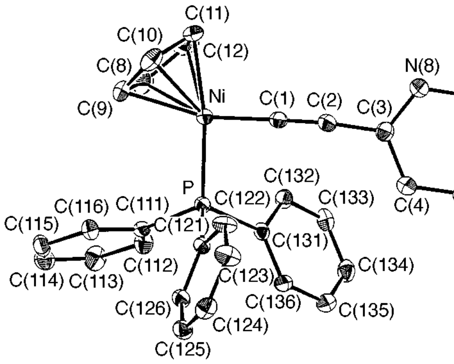

Fig. 1 Molecular structure and atomic labelling scheme for [Ni{2-(C≡C)$C_5H_3NNO_2$-5}(PPh_3)(η-C_5H_5)] **3**. 20% Thermal ellipsoids are shown for the non-hydrogen atoms; hydrogen atoms omitted for clarity

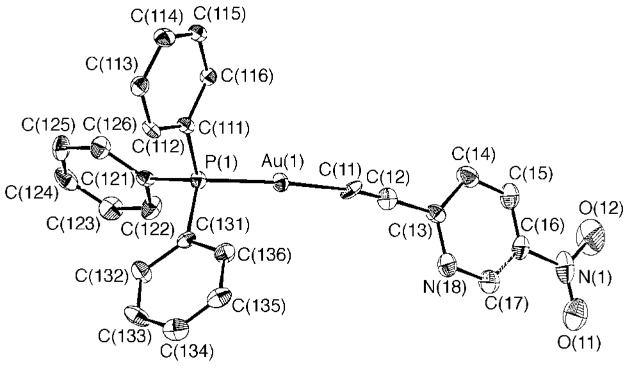

Fig. 2 Molecular structure and atomic labelling scheme for [Au{2-(C≡C)$C_5H_3NNO_2$-5}(PPh_3)] **5**. Details as in Fig. 1

Table 2 Important bond lengths (Å) and angles (°) for complex **3**

Ni–C(1)	1.832(5)	C(7)–N(8)	1.329(6)
C(1)–C(2)	1.215(7)	N(8)–C(3)	1.345(7)
C(2)–C(3)	1.413(7)	C(6)–N(1)	1.458(7)
C(3)–C(4)	1.407(7)	N(1)–O(1)	1.235(6)
C(4)–C(5)	1.355(7)	N(1)–O(2)	1.211(6)
C(5)–C(6)	1.361(7)	Ni–P	2.139(2)
C(6)–C(7)	1.377(7)		
Ni–C(1)–C(2)	175.6(5)	C(1)–C(2)–C(3)	169.5(6)

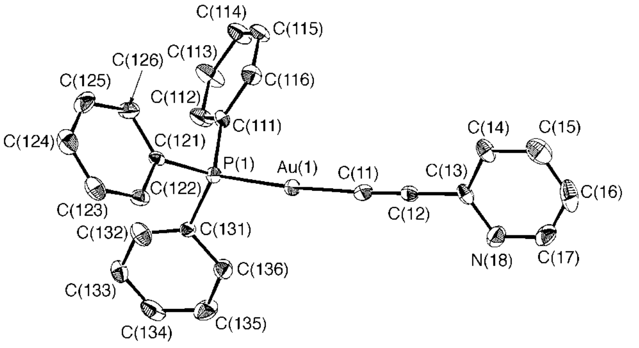

Fig. 3 Molecular structure and atomic labelling scheme for [Au{2-(C≡C)C_5H_4N}(PPh_3)] **6**. Details as in Fig. 1

small 'W' coupling to H^5. The UV/VIS spectra for **1**–**6** contain absorption maxima to lower energy of those of the phenylacetylide analogues. These absorption maxima proceed to lower energy on introduction of a nitro substituent [331 (**2**), *cf.* 468 (**1**); 413 (**4**), *cf.* 456 (**3**); 300 (**6**), *cf.* 339 nm (**5**)].

Crystal structural studies

We have confirmed the identities of complexes **3**, **5** and **6** by carrying out single-crystal X-ray diffraction studies, the first such studies of σ-pyridylacetylide complexes; crystallographic data are collected in Table 1 and selected bond lengths and angles in Tables 2 (**3**) and 3 (**5**, **6**). The ORTEP[17] plots are displayed in Figs. 1 (**3**), 2 [**5**: one independent molecule only, the other two being very similar in geometry (Table 3)], and 3 [**6**: one independent molecule only, the other being very similar in geometry (Table 3)].

The lattice packing of these materials is relevant to analysis of the Kurtz powder measurements below. Complex **3** crystallized in the non-centrosymmetric space group $Pna2_1$. In contrast, **5** and **6** crystallized in centrosymmetric space groups, ensuring that no bulk response would be observed for them. For **3** the Ni–P(1) bond length is normal, being very similar to those reported for [Ni(C≡CPh)(PPh_3)(η-C_5H_5)] and [Ni(C≡CC_6H_4-NO_2-4)(PPh_3)(η-C_5H_5)].[3j] The Ni–C(1)–C(2)–C(3) unit is almost linear, the slight deviation probably arising from pack-

Table 3 Important bond lengths (Å) and angles (°) for complexes **5** and **6**

	5			**6**	
	Molecule 1	Molecule 2	Molecule 3	Molecule 1	Molecule 2
Au(1)–P(1)	2.281(4)	2.276(3)	2.273(3)	2.274(3)	2.263(3)
Au(1)–C(11)	2.01(1)	1.97(1)	1.99(1)	1.97(1)	1.95(1)
C(11)–C(12)	1.08(2)	1.21(2)	1.18(1)	1.21(1)	1.21(1)
C(12)–C(13)	1.50(2)	1.43(2)	1.48(2)	1.45(1)	1.47(1)
C(13)–C(14)	1.41(2)	1.39(2)	1.36(2)	1.36(1)	1.38(1)
C(14)–C(15)	1.38(2)	1.38(2)	1.38(2)	1.38(2)	1.37(1)
C(15)–C(16)	1.32(2)	1.38(2)	1.34(2)	1.38(2)	1.35(1)
C(16)–C(17)	1.37(2)	1.38(2)	1.37(2)	1.36(2)	1.38(1)
C(17)–N(18)	1.33(2)	1.35(1)	1.34(1)	1.31(1)	1.31(1)
N(18)–C(13)	1.33(2)	1.36(2)	1.35(2)	1.35(1)	1.33(1)
C(16)–N(1)	1.46(2)	1.49(2)	1.46(2)	—	—
N(1)–O(11)	1.22(2)	1.23(1)	1.17(2)	—	—
N(1)–O(12)	1.17(2)	1.20(1)	1.26(2)	—	—
P(1)–Au(1)–C(11)	175.0(4)	175.8(4)	178.0(4)	173.9(3)	177.3(3)
Au(1)–C(11)–C(12)	172(2)	174(1)	175(1)	174.9(9)	177(1)
C(11)–C(12)–C(13)	177(2)	176(2)	175(2)	177(1)	177(1)

Table 4 Cyclic voltammetric data for complexes **1**–**4**

Complex		$E°_M$ [a]/V	i_{pc}/i_{pa}	$E°_{NO_2}$ [b]/V	i_{pa}/i_{pc}
1	$[Ru\{2\text{-}(C{\equiv}C)C_5H_3NNO_2\text{-}5\}(PPh_3)_2(\eta\text{-}C_5H_5)]$	0.83	1.0	−0.89	0.9
	$[Ru(C{\equiv}CC_6H_4NO_2\text{-}4)(PPh_3)_2(\eta\text{-}C_5H_5)]$ [c]	0.73	1.0	−1.08	1.0
2	$[Ru\{2\text{-}(C{\equiv}C)C_5H_4N\}(PPh_3)_2(\eta\text{-}C_5H_5)]$	0.69	0.6	—	—
	$[Ru(C{\equiv}CPh)(PPh_3)_2(\eta\text{-}C_5H_5)]$ [c]	0.55	0.7	—	—
3	$[Ni\{2\text{-}(C{\equiv}C)C_5H_3NNO_2\text{-}5\}(PPh_3)(\eta\text{-}C_5H_5)]$	0.92	0.3	−0.84	0.9
	$[Ni(C{\equiv}CC_6H_4NO_2\text{-}4)(PPh_3)(\eta\text{-}C_5H_5)]$ [d]	0.90	0.4	−0.97	0.7
4	$[Ni\{2\text{-}(C{\equiv}C)C_5H_4N\}(PPh_3)(\eta\text{-}C_5H_5)]$	0.80	0.4	—	—
	$[Ni(C{\equiv}CPh)(PPh_3)(\eta\text{-}C_5H_5)]$ [d]	0.81	0.4	—	—

Experiments performed at −50 °C *vs.* Ag–AgCl in dichloromethane with scanning rate 100 mV s^{-1}. Typical peak-to-peak separations: $Ru^{II/III}$, 60–70; $Ni^{II/III}$, 80–90 mV. [a] Switching potential 1.2 V. [b] Switching potential −1.8 V. [c] Ref 3(*a*). [d] Ref. 3(*j*).

ing forces. The bond distances in the Ni–C(1)≡C(2)–C(3) unit are possibly indicative of slightly more Ni^+=C(1)=C(2)=C(3)$^-$ contribution in the ground-state geometry of **3** [Ni–C(1) 1.832(5), C(1)–C(2) 1.215(7), C(2)–C(3) 1.413(7) Å] compared to the analogous phenylacetylide [1.850(3), 1.856(3); 1.193(4), 1.191(4); 1.445(4), 1.437(4) Å for two independent molecules] and 4-nitrophenylacetylide complexes [1.842(6), 1.207(7), 1.422(7) Å], but differences in distances are within 3σ. Gold–phosphine distances in **5** and **6** are close to 2.27 Å, the same as observed for related (triphenylphosphine)gold phenylacetylides.[3g] The variation of the Au(1)–C(11)–C(12)–C(13) bond length data for **5** and **6** allows a direct comparison in the ground-state structures when 5-H is replaced by the strong acceptor 5-NO_2; differences are small, and not consistent with a vinylidene contribution to the 5-NO_2 compound **5**.

Electrochemical studies

As the donor strength of the ligated metal centre is a factor influencing the quadratic non-linearity of these acetylide complexes, ease of oxidation may be related to large hyperpolarizability. The results of cyclic voltammetric investigations of the ruthenium and nickel complexes **1**–**4** are summarized in Table 4, together with data from the analogous phenylacetylide complexes. All complexes undergo one-electron oxidation assigned to the $Ru^{II/III}$ (**1**, **2**) or $Ni^{II/III}$ (**3**, **4**) couple. Replacing pyridylacetylide by the more electron-withdrawing 4-nitropyridylacetylide results in the expected increase in oxidation potential (0.14 V for the ruthenium complexes, 0.12 V for the nickel complexes). Replacing the nitrophenylacetylide ligand by the nitropyridylacetylide ligand leads to an increase of 0.10 V in oxidation potential for the ruthenium complexes, but no significant difference for the nickel complexes. Similarly, replacing phenylacetylide by pyridylacetylide leads to an increase of 0.14 V in oxidation potential for the ruthenium complexes, but no difference with the nickel compounds. Complexes **1** and **3** undergo one-electron reduction at −0.89 and −0.84 V, assigned to reduction of the nitro substituent. As the oxidation waves are associated with metal-centred highest occupied molecular orbitals (HOMOs) and the reduction waves with nitro-centred lowest unoccupied molecular orbitals (LUMOs), ease of electron removal from the donor and addition to the acceptor group may be relevant to the non-linear optical response. We have examined $E°_{M^{II/III}} - E°_{NO_2/NO_2^-}$ for these complexes. For ruthenium, this parameter is 1.72 V for the nitropyridylacetylide complexes and 1.81 V for the nitrophenylacetylide compounds while, for nickel, the values are 1.76 and 1.87 V, respectively. Our comparison of these data is necessarily cautious, given the fact that the $Ru^{II/III}$ and $Ni^{II/III}$ couples are not equally reversible. Nevertheless, if these electrochemical data have predictive merit one should expect to see larger non-linearities for ruthenium than for nickel.

Quadratic hyperpolarizabilities

We have previously determined the molecular quadratic optical non-linearities of ruthenium, nickel and gold σ-phenylacetylide complexes, and have now extended these studies to the σ-pyridylacetylide complexes **1**–**7**. Experimentally obtained data at 1064 nm by hyper-Rayleigh scattering and two-level-corrected values are collected in Table 5, together with related data for analogous σ-phenylacetylide complexes. [Note: the two-state model has been utilized for calculating frequency-independent values, but it may not be adequate for donor–acceptor organometallic systems; it was developed for a restricted class of organic compounds where structural modifications are directed at the charge-transfer band thought to contribute to the hyperpolarizability, and may not be useful where there are several dominant optical transitions close to 2ω.] For **1**–**7** the relative ordering for observed and two-level-corrected β

Table 5 Experimental linear optical spectroscopic and quadratic non-linear optical response parameters

Complex	λ/nm ($\varepsilon/10^4$ dm^3 mol^{-1} cm^{-1})	$\beta_{1064}{}^a/10^{-30}$ esu	$\beta_{corr}{}^b/10^{-30}$ esu
$[\mathrm{Ni(C{\equiv}CPh)(PPh_3)(\eta\text{-}C_5H_5)}]^c$	307 (2.5) (br)	24^c	15
$[\mathrm{Ni(C{\equiv}CC_6H_4NO_2\text{-}4)(PPh_3)(\eta\text{-}C_5H_5)}]^c$	439 (0.9), 368 (1.3)	221	59
4 $[\mathrm{Ni\{2\text{-}(C{\equiv}C)C_5H_4N\}(PPh_3)(\eta\text{-}C_5H_5)}]$	415 (0.1), 327 (1.4) (sh), 305 (2.0)	25	8
3 $[\mathrm{Ni\{2\text{-}(C{\equiv}C)C_5H_3NNO_2\text{-}5\}(PPh_3)(\eta\text{-}C_5H_5)}]$	456 (1.1), 363 (1.1), 308 (1.4)	186	41
$[\mathrm{Ru(C{\equiv}CPh)(PPh_3)_2(\eta\text{-}C_5H_5)}]^d$	310 (2.0)	16	10
$[\mathrm{Ru(C{\equiv}CC_6H_4NO_2\text{-}4)(PPh_3)_2(\eta\text{-}C_5H_5)}]^d$	460 (1.1), 382 (1.1)	468	96
2 $[\mathrm{Ru\{2\text{-}(C{\equiv}C)C_5H_4N\}(PPh_3)_2(\eta\text{-}C_5H_5)}]$	331 (1.4), 308 (1.3)	18	10
1 $[\mathrm{Ru\{2\text{-}(C{\equiv}C)C_5H_3NNO_2\text{-}5\}(PPh_3)_2(\eta\text{-}C_5H_5)}]$	468 (1.7), 286 (1.2) (sh)	622	113
$[\mathrm{Au(C{\equiv}CPh)(PPh_3)}]^e$	296 (1.3), 282 (3.0), 268 (2.7)	6	4
$[\mathrm{Au(C{\equiv}CC_6H_4NO_2\text{-}4)(PPh_3)}]^e$	338 (2.5)	22	12
6 $[\mathrm{Au\{2\text{-}(C{\equiv}C)C_5H_4N\}(PPh_3)}]$	300 (2.1), 292 (2.2), 286 (1.9) (sh)	7	4
5 $[\mathrm{Au\{2\text{-}(C{\equiv}C)C_5H_3NNO_2\text{-}5\}(PPh_3)}]$	339 (2.6)	38	20
7 $[\mathrm{Au\{2\text{-}(C{\equiv}C)C_5H_3NNO_2\text{-}5\}(PMe_3)}]$	340 (1.6)	12	6

All measurements in thf solvent. All complexes are optically transparent at 1064 nm. [a] HRS at 1064 nm; values ±10%. [b] HRS at 1064 nm corrected for resonance enhancement at 532 nm using the two-level model with $\beta_{corr} = \beta_{exp}[1 - (2\lambda_{max}/1064)^2][1 - (\lambda_{max}/1064)^2]$; damping factors not included. [c] Ref. 3(*j*). [d] Ref. 3(*a*). [e] Ref. 3(*g*).

are almost the same. The only deviation is small: β_{1064} for **2** is less than that for **4**, while this ordering is reversed for the corrected data. This is possibly due to significantly larger resonance enhancement for **4** ($\lambda_{max} = 415$ nm) than for **2** ($\lambda_{max} = 331$ nm), accounted for in the two-level correction. The similarity in the trends of the corrected and experimental data suggests that the effects of structural modification on observed non-linearity reflect their effect on intrinsic non-linearity.

Earlier studies with related ruthenium complexes suggested that replacing L = PMe$_3$ by PPh$_3$ in $[\mathrm{Ru(C{\equiv}CC_6H_4NO_2\text{-}4)L_2\text{-}(\eta\text{-}C_5H_5)}]$ leads to a doubling in β_{HRS}.[3b] This datum was substantially resonance enhanced, although the relative ordering was maintained with two-level-corrected values. The gold complexes have λ_{max} much further removed from 2ω (ω = irradiating frequency) and data for **5** and **7** provide an opportunity to assess with more confidence the effect of phosphine replacement. Replacement of PMe$_3$ with PPh$_3$ in proceeding from **7** to **5** results in a tripling of the β value for both experimental and two-level-corrected data. Quadratic non-linearity depends on the donor strength and the length of the π-electron system. The electron-donating strength of PMe$_3$ is greater than that of PPh$_3$. Conversely, the phenyl groups of the PPh$_3$ ligand provide increased π-electron delocalization possibilities compared to that of PMe$_3$. Given the differing merits of each phosphine, it seems that π system length is more important than variation in the donor strength of the coligand for second-order NLO merit in this system.

Our earlier experimental and two-level-corrected data for donor–bridge–acceptor ruthenium, nickel and gold σ-phenylacetylide complexes suggested that the 18-electron, more easily oxidizable ruthenium is a better donor than the 18-electron, less easily oxidizable nickel, which is in turn a better donor than the 14-electron, less oxidizable gold.[3g,i,j] The present studies extend this comparison to the heterocyclic acetylide domain. Comparison of β (both experimentally observed and two-level corrected) across **1**–**7** for an invariant acetylide ligand reveals that the first hyperpolarizability decreases for the ligated metals according to Ru > Ni > Au, consistent with the phenylacetylide results.

The rationale behind the replacement of the phenyl ring by the pyridyl ring in these acetylide complexes is that heterocycles have lower aromatic stabilization energies (benzene, 150; pyridine, 117 kJ mol^{-1} [18]); it should thus be easier energetically to access the important charge-separated excited state which contributes to the non-linearity. Comparison of the experimentally obtained and two-level-corrected values of the phenylacetylide complexes with those of the pyridylacetylide complexes **2**, **4** and **6** reveals no dramatic difference between these systems. In contrast, replacement of nitrophenylacetylide by nitropyridylacetylide results in an increased non-linearity for the ruthenium and gold systems, and possibly to a slight decrease with the nickel complexes (it should be emphasized, though, that values for the nickel complexes **3** and **4** do not differ significantly). Molecular quadratic non-linearities for the ruthenium and nickel nitropyridylacetylides **1** and **3** are substantially resonance-enhanced. In contrast, the λ_{max} (far removed from 2ω) and oscillator strengths of the gold complexes **5** and **6** are very similar, which permits comparison of and comment on the experimentally obtained non-linearities; values are consistent with an increase in β_{HRS} upon replacing phenyl by a heterocyclic bridging unit in acetylide complexes. Further studies with, for example, thienylacetylides (thiophene aromatic stabilization energy: 122 kJ mol^{-1} [18]) would be helpful in this regard.

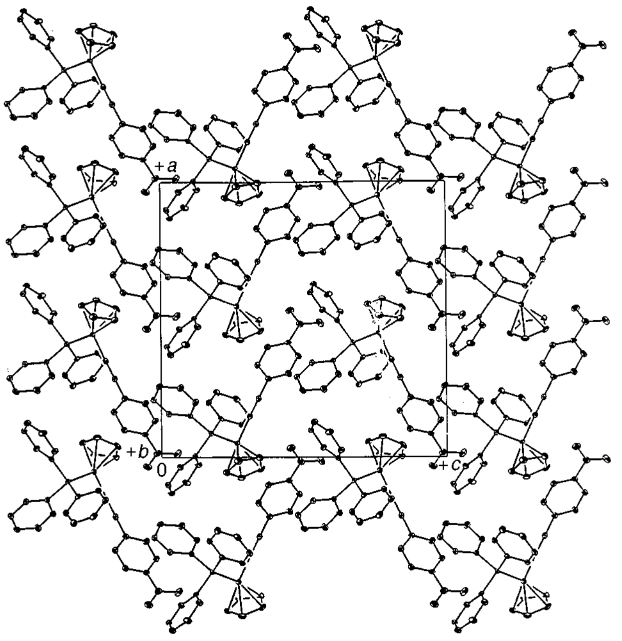

Fig. 4 Cell packing diagram for $[\mathrm{Ni\{2\text{-}(C{\equiv}C)C_5H_3NNO_2\text{-}5\}(PPh_3)\text{-}(\eta\text{-}C_5H_5)}]$ **5** (viewed down the *b* axis and across the *ca* plane)

Powder second harmonic generation (SHG) measurements

Kurtz powder measurements were performed on all σ-pyridylacetylides. A significant response was observed for $[\mathrm{Ni\{2\text{-}(C{\equiv}C)C_5H_3NNO_2\text{-}5\}(PPh_3)(\eta\text{-}C_5H_5)}]$ **3** only, with SHG eight times that of urea; complex **3** is the only one of those synthesized known to have a non-centrosymmetric lattice array. The cell-packing diagram for it is given in Fig. 4. The acetylide chromophores are at an angle of approximately 45° to the adjacent molecule. As the non-linearity observed is the vectorial sum of contributions from each individual molecule, and this is not the alignment which maximizes the bulk response, attention needs to be paid to crystal-engineering strategies to optimize bulk non-linearity. Given favourable crystal engineering, it is likely that other examples from this series of N-heterocyclic acetylide complexes may afford materials with significant bulk non-linearities.

Conclusion

The first structural characterizations of N-heterocyclic metal acetylide complexes are not consistent with an appreciable vinylidene contribution to the ground-state geometry. One example, $[Ni\{2\text{-}(C{\equiv}C)C_5H_3NNO_2\text{-}5\}(PPh_3)(\eta\text{-}C_5H_5)]$ **3**, packs non-centrosymmetrically in the crystal lattice, satisfying an important requirement for observable bulk second-order non-linearity. As the alignment of the molecules in the unit cell for this complex is not the most favourable, larger $\chi^{(2)}$ should be possible with appropriate crystal engineering to enforce optimum molecular alignment in the lattice. Cyclic voltammetry reveals that the $Ni^{II/III}$ couples for the pyridylacetylide complexes are not significantly different from those of the phenylacetylide complexes, but that the ruthenium pyridylacetylide complexes are >0.1 V harder to oxidize than their phenylacetylide analogues. The parameter $E°_{M^{II/III}} - E°_{NO_2/NO_2^-}$ correctly predicts the relative quadratic NLO merits of the ruthenium and nickel complexes, despite the less-than-ideal reversible response for the $Ni^{II/III}$ couple. The HRS results confirm our earlier ordering of ligated metal centres as donor groups, namely $Ru(PPh_3)_2(\eta\text{-}C_5H_5) > Ni(PPh_3)(\eta\text{-}C_5H_5) > Au(PPh_3)$, and are consistent with an increase in non-linearity upon replacement of trimethylphosphine with triphenylphosphine. The present study permits a cautious assessment of the effect upon the molecular quadratic optical non-linearities of metal acetylides of the replacement of a phenylacetylide ligand by a pyridylacetylide group. The optical non-linearity of the nickel nitropyridylacetylide complex is comparable to that of the nickel nitrophenylacetylide compound. However, an increase in non-linearity is observed for the ruthenium and gold complexes when nitropyridylacetylide replaces nitrophenylacetylide. Further studies of the optical non-linearities of organometallic complexes are currently underway.

Acknowledgements

We thank the Australian Research Council (M. G. H.), the Belgian Government (Grant No. IUAP-P4-11) (A. P.), the Fund for Scientific Research-Flanders (Grant No. G.0308.96) (A. P.), the Institute of Advanced Studies (G. A. H.), the University of Leuven (Grant No. GOA 95/1) (A. P.), and the Flemish Institute of Advancement of the Scientific and Technological Research in Industry (C. B.) for support of this work, and Johnson-Matthey Technology Centre (M. G. H.) for the loan of ruthenium salts. M. P. C. holds an ARC Australian Postdoctoral Research Fellowship, M. G. H. an ARC Australian Research Fellowship, and S. H. is a Research Assistant of the Fund for Scientific Research-Flanders .

References

1 Part 12, I. R. Whittall, M. G. Humphrey, M. Samoc, B. Luther-Davies and D. C. R. Hockless, *J. Organomet. Chem.*, in the press.

2 H. S. Nalwa, *Appl. Organomet. Chem.*, 1991, **5**, 349; S. R. Marder, in *Inorganic Materials*, eds. D. W. Bruce and D. O'Hare, Wiley, Chichester, 1992, p. 115; N. J. Long, *Angew. Chem.*, *Int. Ed. Engl.*, 1995, **34**, 21; I. R. Whittall, A. M. McDonagh, M. G. Humphrey and M. Samoc, *Adv. Organomet. Chem.*, in the press.

3 (*a*) I. R. Whittall, M. G. Humphrey, D. C. R. Hockless, B. W. Skelton and A. H. White, *Organometallics*, 1995, **14**, 3970; (*b*) I. R. Whittall, M. G. Humphrey, A. Persoons and S. Houbrechts, *Organometallics*, 1996, **15**, 1935; (*c*) I. R. Whittall, M. G. Humphrey, M. Samoc, J. Swiatkiewicz and B. Luther-Davies, *Organometallics*, 1995, **14**, 5493; (*d*) A. M. McDonagh, I. R. Whittall, M. G. Humphrey, B. W. Skelton and A. H. White, *J. Organomet. Chem.*, 1996, **519**, 229; (*e*) A. M. McDonagh, I. R. Whittall, M. G. Humphrey, D. C. R. Hockless, B. W. Skeleton and A. H. White, *J. Organomet. Chem.*, 1996, **523**, 33; (*f*) A. M. McDonagh, M. P. Cifuentes, I. R. Whittall, M. G. Humphrey, M. Samoc, B. Luther-Davies and D. C. R. Hockless, *J. Organomet. Chem.*, 1996, **526**, 99; (*g*) I. R. Whittall, M. G. Humphrey, S. Houbrechts, A. Persoons and D. C. R. Hockless, *Organometallics*, 1996, **15**, 5738; (*h*) I. R. Whittall, M. G. Humphrey, M. Samoc and B. Luther-Davies, *Angew. Chem.*, 1997, **109**, 386; *Angew. Chem.*, *Int. Ed. Engl.*, 1997, **36**, 370; (*i*) I. R. Whittall, M. P. Cifuentes, M. G. Humphrey, B. Luther-Davies, M. Samoc, S. Houbrechts, A. Persoons, G. A. Heath and D. C. R. Hockless, *J. Organomet. Chem.*, in the press; (*j*) I. R. Whittall, M. P. Cifuentes, M. G. Humphrey, B. Luther-Davies, M. Samoc, S. Houbrechts, A. Persoons, G. A. Heath, D. Bogsanyi and D. C. R. Hockless, *Organometallics*, 1997, **16**, 2631; (*k*) S. Houbrechts, K. Clays, A. Persoons, V. Cadierno, M. P. Gamasa, J. Gimeno, I. R. Whittall and M. G. Humphrey, *Proc. SPIE-Int. Soc. Opt. Eng.*, 1996, **2852**, 98; (*l*) M. G. Humphrey, *Chem. Aust.*, 1996, **63**, 442; (*m*) S. Houbrechts, K. Clays, A. Persoons, V. Cadierno, M. P. Gamasa and J. Gimeno, *Organometallics*, 1996, **15**, 5266.

4 C. W. Dirk, H. E. Katz, M. L. Schilling and L. A. King, *Chem. Mater.*, 1990, **2**, 700.

5 L.-T. Cheng, W. Tam, S. R. Marder, A. E. Steigman, G. Rikken and C. W. Spangler, *J. Phys. Chem.*, 1991, **95**, 10 643.

6 A. K.-Y. Jen, V. P. Rao, K. Y. Wong and K. J. Drost, *J. Chem. Soc.*, *Chem. Commun.*, 1993, 90.

7 D. F. Shriver and M. A. Drezdzon, *The Manipulation of Air Sensitive Compounds*, Wiley, New York, 1986.

8 T. Sakamoto, M. Shiraiwa, Y. Kondo and H. Yamanka, *Synthesis*, 1983, 312.

9 K. W. Barnett, *J. Chem. Educ.*, 1974, **51**, 422.

10 M. I. Bruce, C. Hameister, A. G. Swincer and R. C. Wallis, *Inorg. Synth.*, 1982, **21**, 78.

11 R. F. Heck, *Palladium Reagents in Organic Syntheses*, Academic Press, London, 1985, p. 18.

12 M. I. Bruce, B. K. Nicholson and O. B. Shawkataly, *Inorg. Synth.*, 1989, **26**, 324.

13 M. I. Bruce, E. Horn, J. G. Matisons and M. R. Snow, *Aust. J. Chem.*, 1984, **37**, 1163.

14 Single Crystal Structue Analysis Software, Version 1.6c, Molecular Structure Corporation, The Woodlands, TX, 1993.

15 M. Stähelin, D. M. Burland and J. E. Rice, *Chem. Phys. Lett.*, 1992, **191**, 245.

16 K. Clays and A. Persoons, *Rev. Sci. Instrum.*, 1992, **63**, 3285; E. Hendrickx, C. Dehu, K. Clays, J. L. Brédas and A. Persoons, *ACS Symp. Ser.*, 1995, **601**, 82; S. Houbrechts, K. Clays, A. Persoons, Z. Pikramenou and J.-M. Lehn, *Chem. Phys. Lett.*, 1996, **258**, 485.

17 C. K. Johnson, ORTEP, Report ORNL-5138, Oak Ridge National Laboratory, Oak Ridge, TN, 1976.

18 T. L. Gilchrist, *Heterocyclic Chemistry*, Pitman, London, 1985.

Received 2nd *April* 1997; *Paper* 7/02249B